



6-6-13

## STEEL FIBER REINFORCED DUCTILE JOINTS

Ioan OLARIU<sup>1</sup>, Adrian IOANI<sup>2</sup>, Nicolae POIENAR<sup>1</sup>

<sup>1</sup> Polytechnic Institute Cluj-Napoca, Cluj-Napoca, Romania

<sup>2</sup> Central Building Research Institute, Department of  
Cluj-Napoca, Cluj-Napoca, Romania

### SUMMARY

Six beam-column joints made with different volumetric percentages of steel fiber reinforcement are presented, compared to two classically reinforced concrete joints, under reversed cyclic loading. An analysis of the positive influence of SFRC on: the stiffness and ultimate strength of the joint, the cracking, final ductility, the energy dissipation capacity and the bond of the bars in SFRC is made.

### INTRODUCTION

Our tests as well as other results (Ref. 1,2,3) mentioned in literature have confirmed the superior characteristics of the SFRC versus plain concrete regarding the tensile strength  $R_{ti}$ , the compressive strength  $R_c$ , the shear strength and the energy absorption under static and mostly under dynamic loading. Starting from the advantages of SFRC and from the necessary requirements of the joints in framed structures built in seismic zones, we have developed an experimental program to study the behaviour of the subassemblages beam-joint-column, where the joint was cast with different volumetric percentages of SFRC, and the reinforcement of the joint was simplified by eliminating a number of stirrups. We have studied the way of cracking, the loss of stiffness under reversed cyclic loading, the ductility of the joint, the energy dissipation capacity, and the bond of the reinforcement in SFRC.

### EXPERIMENTAL PROGRAM

We have cast 8 subassemblages beam-joint-column so that the column should be stronger than the beam and the plastic hinge should appear in the beam. The proof elements ( $F_o, F_{ol}$ ) were made of reinforced concrete, according to the Romanian antiseismic building code P 100-81. The rest of 6 subassemblages were reinforced similarly to the proof ones, but the joint was achieved with different volumetric percentages  $\gamma_v$  of SFRC as it can be observed in Fig.1 and 2. The use of SFRC permitted the reduction of the transverse reinforcement with 3 stirrups without surpassing the maximum

allowable distance, as it is seen in Fig.2.

Materials and testing The characteristics of the concrete used in the subassemblages and of the SFRC in the joint are presented in Table 1. The used steel fiber is stright, round and stainless with  $d=0.38$  mm,  $l=25-30$  mm, the tensile strength  $1200$  N/mm<sup>2</sup>.

Table 1

Element	Fo, Fol	F1, F2	F3	F4	F5	F6
$\checkmark v$ %	-	0.50	0.75	1.00	1.25	1.50
Re N/mm <sup>2</sup>	46.70	45.90	47.80	48.00	50.50	51.50
Rti N/mm <sup>2</sup>	3.15	3.98	4.49	4.53	4.80	4.95

The elements were fixed in the stand and loaded at the end of the beam with a reversed force P as in Fig.3 and 4. The magnitude of the force P was determined by some prestablished ductility factors  $\Delta i$  defined as the ratio between the rotation  $\theta i$  of the section corresponding to a certain force and the rotation  $\theta y$  of the section which led to the yielding of the reinforcement of the beam, in the respective section. The devices C1 and C2 equipped with strain gauges enable the reading of the rotation  $\theta i$  of the beam on a base of 20 cm, as in Fig.3 and 4.

#### TEST RESULTS

In Fig.3 and 4 the cracking pattern for an element Fo ( $\checkmark v=0$ ) and F6 ( $\checkmark v=1.5\%$ ) respectively. In the classical joints (Fo, Fol) and in those with a small content of fiber ( $\checkmark v=0.5\%$ ; F1, F2) the cracking appears in the first cycles; there are diagonal cracks which open themselves severely in the stages of advanced loading, confirming the classical failure mechanism. Contrary to this way of cracking, in the elements with higher percentages of fiber (F4, F5, F6) the cracks appear later, they are finer and mainly distributed on the exterior shape of the joint (Fig.4).

The higher stiffness of the SFRC joint versus the classical joints (Fo, Fol) remains even after a large number of cycles ( $n=11, 12, 13$ ), being more pregnant for moderate loading ( $P=3000$  daN= $0.5P_u$ ,  $P_u$ =ultimate applied loading) as it can be observed in Table 2.

Table 2

Parameters		Rotation $\theta_{max}$ [rad.10 <sup>-4</sup> ]					
Cycle	P [daN]	Fo	F1	F3	F4	F5	F6
n= 5	P=3000	35	25	14	17	12	15
n=11	5000	55	52	40	45	40	40
n=12	4500	62	57	45	48	40	38
n=13	5500	95	87	70	80	80	83
Failure force [daN]		5700	5850	6100	6000	6350	6500

The ultimate strength capacity of the joints increases with the use of SFRC - as it can be seen in Tab.2 - due to the higher quality of the concrete in the joint and to the better bond and anchorage of the bars crossing the SFRC core. The bond tests made on steel bars with different diameters, anchored in normal concrete and in SFRC, pointed out the favourable influence of steel fiber reinforcement on the unitary bond stress  $\bar{\sigma}_{max}$  as function of the reinforcement type and of the fiber content of the concrete.

The results of the bond tests are presented in Table 3.

Table 3

Parameters	Unitary bond stress $\bar{\sigma}_{max}$ [N/mm <sup>2</sup> ]		
SFRC with $\gamma_v$ %	0.0	1.0	1.5
Diameter of bar $\phi=16$ mm	8.6	9.2	9.5
$\phi=18$ mm	9.5	12.0	16.0
$\phi=22$ mm	7.7	10.0	12.1

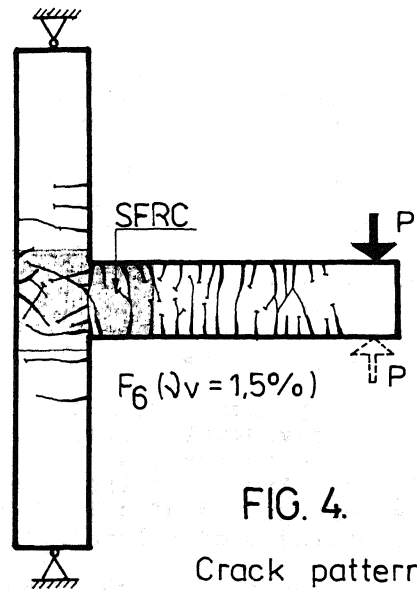
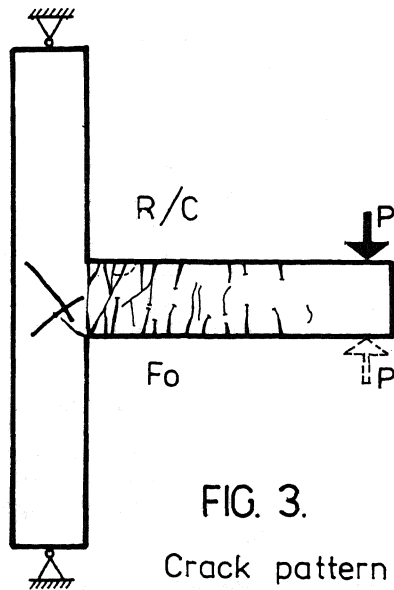
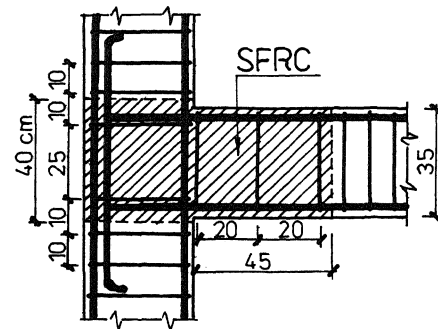
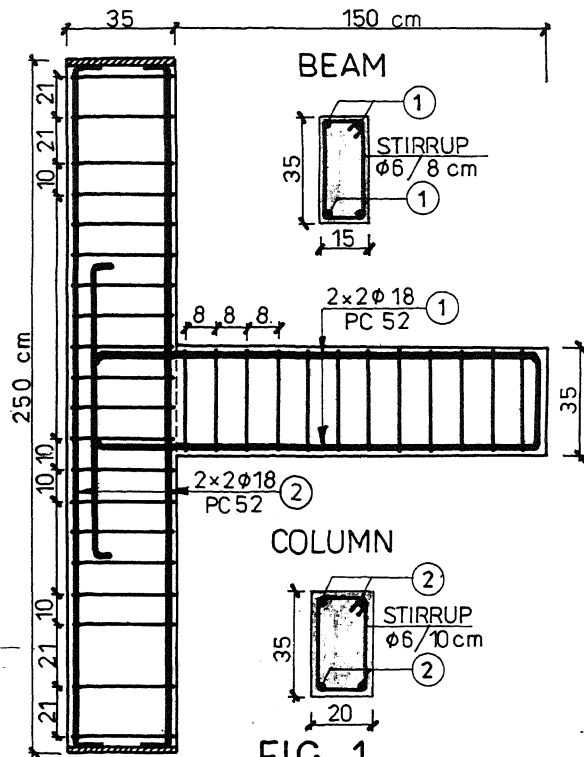
The hysteretic loops (M- $\theta$ ) for all subassemblages were drawn after a preestablished loading history presented in Fig.5 and 6. Important changes in the shape of the loops are observed as function of the increase of the fiber content as well as the larger ductility of the fiber joints in the limit cycle  $n=13$  (Fig.7). The increase of the ultimate ductility factor, illustrated in Fig.8, is a consequence of the superior confinement, ensured by the cracks, hinders the splitting of concrete and improves the bond of the anchored bars even at relatively great strains and at a great number of cyclic reversed loadings. In Fig.9 and 10 we present the important increase in the energy dissipation, in the last cycle as well as in the ensemble of the cycles, as function of the increase of the steel fiber content in the joint.

#### CONCLUSIONS

After the tests we can draw the following conclusions:

- The working and failure mechanism of the SFRC joints - for percentages of volumetric reinforcement  $\gamma_v > 1\%$  - is different from the classical one and favourable for seismic loading. The joint has an improved stiffness and strength, there are several fine cracks which do not lead to the splitting or crushing of concrete (Fig.3,4).
- The bond of the longitudinal bars is improved leading to their better anchorage in the SFRC core. The increase in the unitary bond stress  $\bar{\sigma}_{max}$  is up to 30% for SFRC with  $\gamma_v=1\%$  and up to 60% for SFRC with  $\gamma_v=1.5\%$  for  $\phi=22$  mm (Tab.3).
- The ultimate ductility factor increase with the fiber content (Fig.7). This is relevant because the tested subassemblage F4, at which the total used steel (bars and fiber) was greater with 3% versus the element without fiber F0, and the ductility increase was of 30% (Fig.8). We have to mention that the ductility does not increase linearly with the fiber content, and for this reason we consider the optimal volumetric reinforcement percentage  $\gamma_v$  for frame joints as being between 1-1.5%.
- The energy dissipation capacity is much improved by the use of SFRC, the favourable influence of the steel fiber content being more visible in the last cycles (increases of 10% - F6 versus F1 - in Fig.9). After all the loading cycles the increase of the dissipated energy was of 46% (F6 versus F0 in Fig.10) being important for percentages of volumetric reinforcement of 1-1.5%.

Starting from these encouraging results we are working on a research program to introduce the SFRC in the frame joints of precast reinforced concrete structures used in seismic areas.



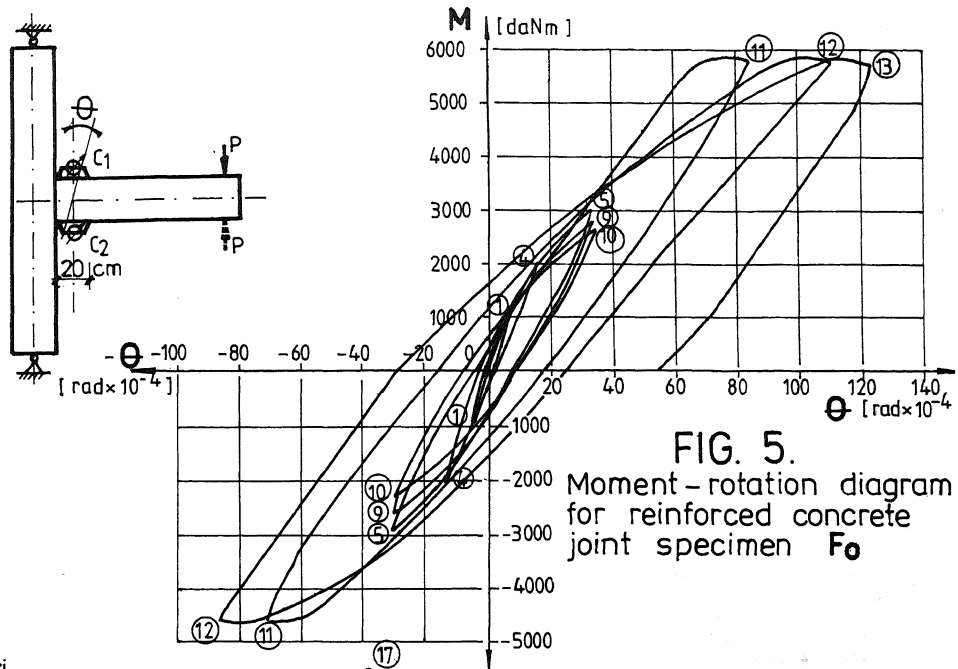


FIG. 5.  
Moment-rotation diagram  
for reinforced concrete  
joint specimen  $F_0$

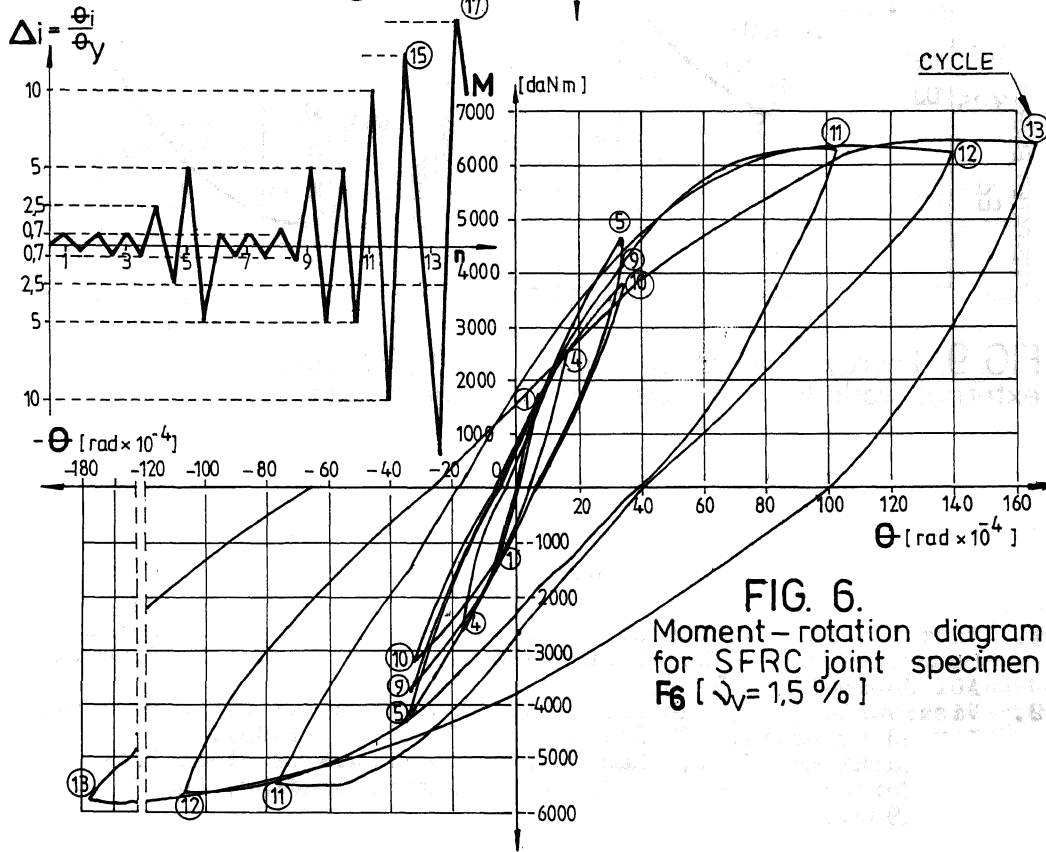


FIG. 6.  
Moment-rotation diagram  
for SFRC joint specimen  
 $F_6$  [ $\rho_v = 1.5\%$ ]

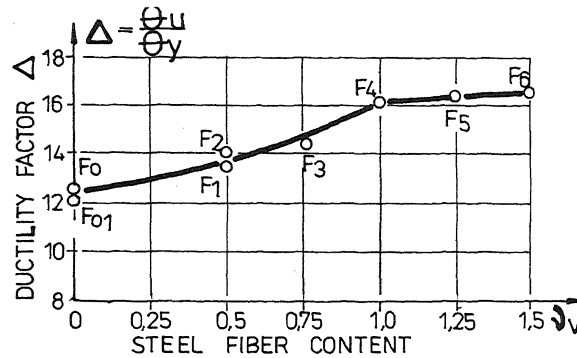


FIG. 7. Effect of steel fiber content on ductility factor  $\Delta$

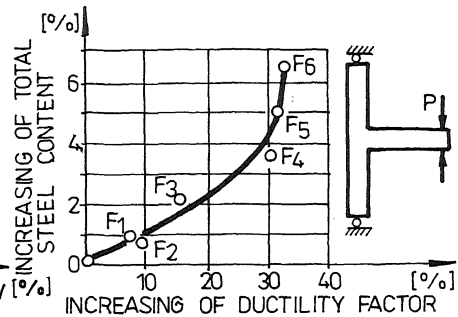


FIG. 8. Variation of ductility

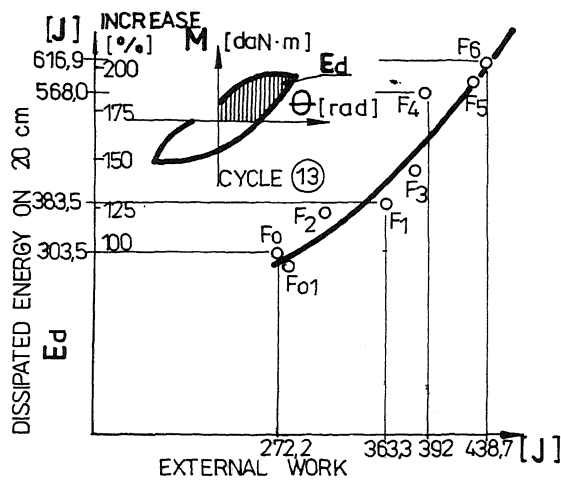


FIG. 9. Energy dissipation versus external work for each specimen

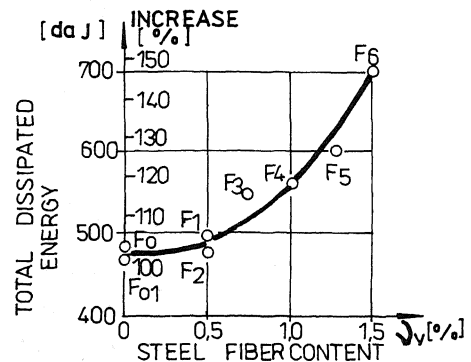


FIG. 10. Total dissipated energy versus steel fiber content

#### REFERENCES

1. Patton, M.N., Whittaker, W.L., Effects of Fiber Content and Damaging Load on Steel Fiber Reinforced Concrete Stiffness, ACI Journal, 1, 13-16, (1983).
2. Visalvanich, K., Naaman, A.E., Fracture Model for Fiber Reinforced Concrete, ACI Journal, 2, 128-138, (1983).
3. Gopalaratnam, V.S., Shah, S.P., Properties of Steel Fiber Reinforced Concrete Subjected to Impact Loading, ACI Journal, 1, (1986).